Available online at www.derpharmachemica.com

ISSN 0975-413X
CODEN (USA): PCHHAX

Der Pharma Chemica, 2016, 8(2):380-391
(http://derpharmachemica.com/archive.html)

Relationship between structure and inhibition behaviour of (E)-4-(2,3-Dihydro-1,3-benzothiazol-2-ylidene)-3-methyl-1-phenyl-1H-pyrazol-5(4H)-one (P1) for mild steel corrosion: Experimental and theoretical approach

I. Chakib[1], H. Elmsellem[2], N. K. Sebbar[1], E. M. Essassi[1], I. Fichtali[3], A. Zerzouf[4], Y. Ouzidan[3], A. Aouniti[2], B. El Mahi[2] and B. Hammouti[2]

[1]Laboratoire de Chimie Organique Hétérocyclique, URAC 21, Pôle de Compétences Pharmacochimie, Université Mohammed V, Faculté des Sciences, Av. Ibn Battouta, Rabat, Morocco
[2]Laboratoire de Chimie Appliquée et environnement (LCAE-URAC18), Faculté des Sciences, Oujda, Morocco
[3]Laboratoire de Chimie Organique Appliquée, Université Sidi Mohamed Ben Abdallah, Faculté des Sciences et Techniques, Route d'Immouzzer, Fez, Morocco
[4]Laboratoire de Chimie Organique et Etudes Physicochimiques, ENS Takaddoum, Université Mohammed V, Rabat, Morocco

---

ABSTRACT

*Corrosion inhibition behaviour of (E)-4-(2,3-Dihydro-1,3-benzothiazol-2-ylidene)-3-methyl-1-phenyl-1H-pyrazol-5(4H)-one **(P1)** on mild steel corrosion in 1 M HCl was investigated at various concentrations by gravimetric and electrochemical techniques. The polarization curves indicated that (E)-4-(2,3-Dihydro-1,3-benzothiazol-2-ylidene)-3-methyl-1-phenyl-1H-pyrazol-5(4H)-one **(P1)** as mixed inhibitor. The adsorption of (E)-4-(2,3-Dihydro-1,3-benzothiazol-2-ylidene)-3-methyl-1-phenyl-1H-pyrazol-5(4H)-one **(P1)** on mild steel leading to inhibition was found to follow the Langmuir adsorption isotherm. The quantum chemical calculations were carried out to establish the mechanism of corrosion inhibition.*

Key words: (E)-4-(2,3-Dihydro-1,3-benzothiazol-2-ylidene)-3-methyl-1-phenyl-1H-pyrazol-5(4H)-one, Mild steel, Polarization, EIS, Acid corrosion, DFT.

INTRODUCTION

Mild steel, the most widely used engineering material, despite its relatively limited corrosion resistance used in large tonnages in marine applications, nuclear powered transportation, chemical processing, petroleum production and refining, pipelines, mining, construction and metal-processing equipment [1-4]. The inhibition of mild steel corrosion of iron in acidic media by different organic compounds has been widely studied [5-7]. The existing literature shows that most of the organic inhibitors act by getting adsorbed on the iron surface. This phenomenon is influenced by the nature and surface charge on metal, the type of aggressive electrolyte and the chemical structure of inhibitor[8-10].The use of organic inhibitors is one of the most practical methods for protection of metals against corrosion, and is becoming increasingly popular according to recent studies[11-13]. The inhibitory efficiency of organic molecules mainly depends on their adsorption ability on metal surface, which can markedly change the corrosion resisting properties of metals [14-17]. The adsorption of organic molecules on metals surfaces depends mainly on the nature and the surface charge of metals, the chemical structure of organic molecule (functional groups, steric factors, electron density, etc.) and the type of solution [18-22]. Benzothiazole derivatives possess a wide spectrum of biological and pharmacological activities due to presence of a fold along the nitrogen and sulfur axis, which is considered to be responsible as one of the structural features to impart their activities [23-24]. The synthesis of novel benzothiazole derivatives and investigation of their chemical and biological behaviour have

gained more importance in recent decades for medicinal and agricultural reasons. Different classes of benzothiazole derivatives possess an extensive spectrum of pharmacological activities, particularly in compounds bearing benzothiazoles which are known to exhibit unique anti-HIV activity [25]. Substituted benzothiazole moieties has been found to have important activities such as antimalarial[26], anti-microbial[27-28], anti-diabetic [29] etc. Furthermore pyrazole derivatives occupy an important position in medicinal chemistry due to their wide of bioactivities such as antiparisitaires [30], anti-inflammatory [31], antitumor [32], etc. All these properties have motivated us to synthesize a compound with two entities benzothiazoles and pyrazole in the same structure (E)-4-(2,3-Dihydro-1,3-benzothiazol-2-ylidene)-3-methyl-1-phenyl-1H-pyrazol-5(4H)-one **(P1) Scheme 1**.

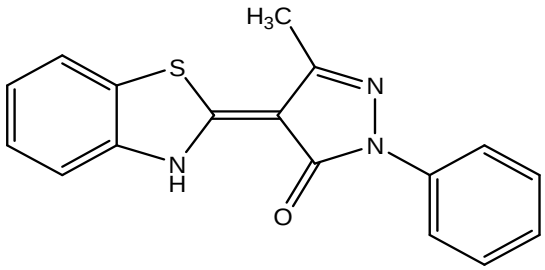

Scheme 1: (E)-4-(2,3-Dihydro-1,3-benzothiazol-2-ylidene)-3-methyl-1-phenyl-1H-pyrazol-5(4H)-one (P1) [33]

The investigation on the inhibition effect of synthesized (E)-4-(2,3-Dihydro-1,3-benzothiazol-2-ylidene)-3-methyl-1-phenyl-1H-pyrazol-5(4H)-one **(P1)**, on the corrosion of mild steel in 1 M HCl was performed by gravimetry, potentiodynamic polarization and electrochemical impedance spectroscopic (EIS) measurements. The effect of concentration on the inhibition efficiencies of P1 has been systematically studied. In addition to this, quantum chemical calculations were performed to add theoretical support to the experimental results.

MATERIALS AND METHODS

2.1. Materials and sample preparation

The composition (wt.%) of mild steel samples used for all the experiments was as follows: C = 0.253; Si = 0.12; P = 0.013; S = 0.024; Cr = 0.012; Mn = 0.03 and balance Fe. Coupons cut into 1.5 x 1.5 x 0.05 cm size were used for gravimetric measurements where as specimens of size with 1 cm2 exposed surface areas were used as working electrode for polarization and EIS measurements. Before starting the experiments, the specimens were mechanically abraded with 320, 400, 600, 800, 1000 and 1200 grade of emery papers. These were then degreased with acetone, washed with double distilled water and dried in air before immersing in the corrosive medium.

The corrosive solution, 1.0 M HCl was prepared by dilution of analytical grade HCl of predetermined normality with triple distilled water. The concentration range of P1 used was 10-6 M to 10-3 M. The volume of electrolyte used in each experiment was 100 mL.

2.2. Synthesis of inhibitors

In a 100 ml flask was added (0.014 mole) of 2-aminothiophenol, and (0.0025 mole) of 5- [1-phenyl-3-methyl-5-oxo-pyrazol-4-ylidene]-1.7-dimethyl-3-phénylpyrano[2,3-c]pyrazole in n-butanol (50 mL). The mixture is refluxed for three days. The product (E)-4-(2,3-Dihydro-1,3-benzothiazol-2-ylidene)-3-methyl-1-phenyl-1H-pyrazol-5(4H)-one **(P1)** was precipitated first in n-butanol with a yield of 60% (M.p 461-462K); a second compound with the bipyrazole structure was isolated with a low yield **Scheme 2**.

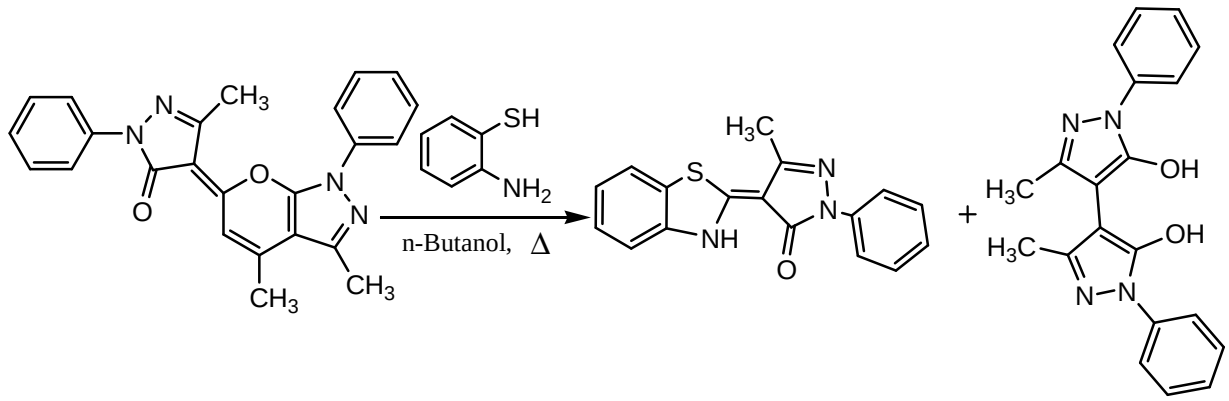

Scheme 2: Synthesis of (E)-4-(2,3-Dihydro-1,3-benzothiazol-2-ylidene)-3-methyl-1-phenyl-1H-pyrazol-5(4H)-one (P1)

The analytical and spectroscopic data are conforming to the structure of compound **(P1)** formed.

(P1):**Yield** = 60%; **M.p.** 461-462K; **RMN^{1}H (DMSO-d6) δ ppm :** 9.7(s,1H,HN), 2.4 (S,3H,CH_3), 7.16 -8.002(m, 9H,H-ar); **RMN^{13}C (DMSO-d6) δ ppm :** 14.81 (CH_3), 161.79 (C=O), 146.111 ;140.713 ; 138.743 ; 126.00 ; 115.264 ; 96.435 (Cq), 128.991 ; 128.825 ; 127.834 ; 124.847 ; 124.579 ; 122.095 ; 119.472 ; 115.261 (CH ar).

2.3. Experimental techniques

2.3.1. Gravimetric measurements

Finely abraded and dried mild steel specimens of dimension 1.5 x 1.5 x 0.05 cm were weighed on a digital balance with 1 mg sensitivity and immersed for 6 h in 1 M HCl at 308 K in the absence and presence of 10^{-6} M to 10^{-3} M of P1. The immersion time of 6 h was selected because the corrosion rate attends its limiting value. In all the above measurements, at least three closer results were considered for taking the average values.
The percent inhibition, E% for the weight loss method, is calculated as follows:

$$E\ (\%) = \frac{W0 - Wi}{W0} \text{x } 100 \qquad \textbf{(1)}$$

w_i and w_0 are the corrosion rates of steel samples with and without inhibitor, respectively.

2.3.2. Electrochemical measurements

Electrochemical impedance spectroscopic (EIS) studies and potentiostatic polarization studies were carried out using a potentiostat PGZ100 piloted by Voltamaster soft-ware. This potentiostat is connected to a cell with three electrode thermostats with double wall. The mild steel specimens used as working electrode while platinum and calomel electrodes were used as counter electrode and the reference electrode, respectively. Impedance measurements were carried out at E_{corr} potential at the range of 100 kHz to 10 MHz at amplitude of 10 mV. The impedance diagrams are given in Nyquist representation. The impedance and polarization parameters such as double layer capacitance (C_{dl}), charge transfer resistance (R_{ct}), corrosion current (I_{corr}), corrosion potential (E_{corr}), anodic Tafel slope (βa) and cathodic Tafel slope (βc) were computed from the polarization curves and Nyquist plots. The Ep values were calculated from potentiodynamic polarization measurements using the equation (2).

$$E_p\,\% = \frac{I_{corr(o)} - I_{corr(inh)}}{I_{corr(o)}} \text{ X } 100 \qquad \textbf{(2)}$$

Where $I_{corr(0)}$ and I_{corr} are current density in absence and presence of (E)-4-(2,3-Dihydro-1,3-benzothiazol-2-ylidene)-3-methyl-1-phenyl-1H-pyrazol-5(4H)-one **(P1)**, respectively.

The inhibition efficiency got from the charge-transfer resistance is calculated by the following relation:

$$E_{Rt}\,\% = \frac{R_{t(inh)} - R_{t(o)}}{R_{t(inh)}} \text{x } 100 \qquad \textbf{(3)}$$

Where $R_{t(0)}$and $R_{t(inh)}$ are the charge transfer resistance values in the absence and presence of inhibitor, respectively.

2.4. Quantum chemical calculations

All quantum chemical study was carried out using the Density Functional Theory (DFT) with hybrid functional B3LYP, based on Becke's three-parameter functional including Hartree–Fock exchange contribution with a nonlocal correction for the exchange potential proposed by Becke [34-35] together with the nonlocal correction for the correlation energy provided by Lee et al. [36]. Since electrochemical corrosion takes place in liquid phase, and for a better approach of the experimental results, we used the Self-Consistent Reaction Field (SCRF) theory [36], with Tomasi's Polarized Continuum Model (PCM) [37], to include the effect of solvent in the computations. This approach models the solvent as a continuum of uniform dielectric constant (ε) and defines the cavity where the solute is placed as a uniform series of interlocking atomic spheres.

The quantum chemical investigations were used to look for good theoretical parameters to be correlated with the inhibitive performance of the studied benzothiazoles and pyrazole derivatives. To do so, some of molecular properties, describing the global reactivity such as: the energy of the Highest Occupied Molecular Orbital (E_{HOMO}), the energy of the Lowest Unoccupied Molecular Orbital (E_{LUMO}), the energy gap ($\Delta E=E_{LUMO}-E_{HOMO}$), the electrical dipole moment (μ), the Ionization Potential (IP), the Electron Affinity (EA), the electronegativity (χ), the global hardness (η) and were calculated. Other parameters describing the local selectivity of the studied molecules such as the local natural populations and the Fukui functions were also considered. In order to estimate some of the previous descriptors, the Koopmans' theorem was used [38] to relate the HOMO and LUMO energies to the IP and EA, respectively:

$$IP = -E_{HOMO} \quad \textbf{(4)}$$

$$EA = -E_{LUMO} \quad \textbf{(5)}$$

Then the electronegativity and the global hardness were evaluated, based on the finite difference approximation, as linear combinations of the calculated IP and EA.

$$\chi = \frac{IP + EA}{2} \quad \textbf{(6)}$$

$$\eta = \frac{IP - EA}{2} \quad \textbf{(7)}$$

RESULTS AND DISCUSSION

3.1. Effect of inhibitor P1 concentration

3.1.1. Gravimetric measurements

It is evident from the data recorded in Table 1 that the corrosion rate decreases and the inhibition efficiency (E_w) increases with increasing inhibitor concentration reaching a maximum value of 94% at a concentration of 10^{-3}M. These results indicate that this (E)-4-(2,3-Dihydro-1,3-benzothiazol-2-ylidene)-3-methyl-1-phenyl-1H-pyrazol-5(4H)-one **(P1)** inhibitor can effectively prevent mild steel from dissolving in the acidic media probably through their adsorption at the mild steel surfaces.

Table 1. Corrosion parameters obtained from weight loss measurements for mild steel in 1 M HCl containing various concentrations of (E)-4-(2,3-Dihydro-1,3-benzothiazol-2-ylidene)-3-methyl-1-phenyl-1H-pyrazol-5(4H)-one (P1) at 308 K

Inhibitor	Concentration (M)	C_R ($mg.cm^{-2}h^{-1}$)	Ew (%)	θ
HCl 1M	--	0.82	--	--
Inhibitor (P1)	10^{-6}	0.23	72	0.72
	10^{-5}	0.11	87	0.87
	10^{-4}	0.07	91	0.91
	10^{-3}	0.05	94	0.94

3.2. Electrochemical Impedance Studies

Nyquist plots for mild steel immersed in 100 mL of solution in the absence and presence of (E)-4-(2,3-Dihydro-1,3-benzothiazol-2-ylidene)-3-methyl-1-phenyl-1H-pyrazol-5(4H)-one **(P1)** are shown in Figure 1. The impedance parameters, charge transfer resistance (R_{ct}), Double layer capacitance (C_{dl}) from the Nyquist plot values are shown in Table 2.

When mild steel is immersed in 100 mL HCl medium the R_{ct} value is found to be 14.50 (Ω cm^2). The C_{dl} value is 200 ($\mu F/cm^2$). When 10^{-6} M P1 to of 10^{-3} M the R_{ct} value has increased from 71 to 439 (Ω cm^2) and the C_{dl} value has decreased from 92 to 35 ($\mu F/cm^2$). The increase in R_{ct} values and decrease in double layer capacitance values obtained from impedance studies justify the good performance of a (E)-4-(2,3-Dihydro-1,3-benzothiazol-2-ylidene)-3-methyl-1-phenyl-1H-pyrazol-5(4H)-one **(P1)** as an inhibitor in HCl medium. This behavior means that the film obtained acts as a barrier to the corrosion process that clearly proves the formation of the film.

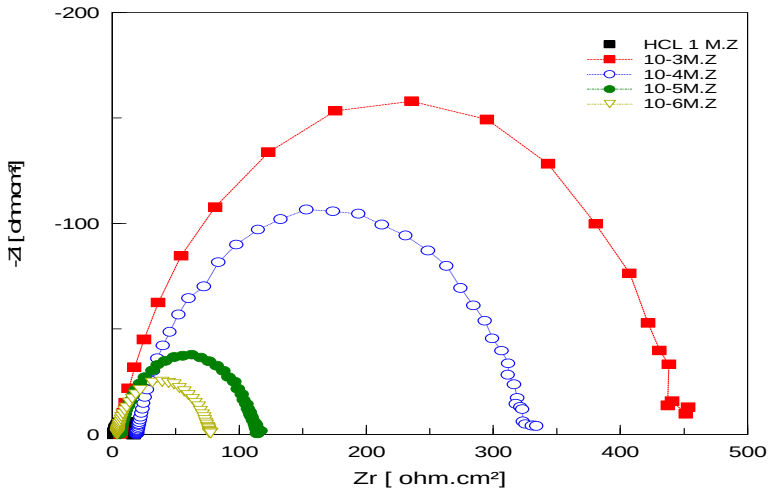

Figure 1. Electrochemical impedance curves of mild steel in 1M HCl without and with different concentrations (E)-4-(2,3-Dihydro-1,3-benzothiazol-2-ylidene)-3-methyl-1-phenyl-1H-pyrazol-5(4H)-one (P1)

Table 2. Impedance parameters and inhibition efficiency values for mild steel after 1/2 h immersion period in 1 M HCl containing different concentrations of (E)-4-(2,3-Dihydro-1,3-benzothiazol-2-ylidene)-3-methyl-1-phenyl-1H-pyrazol-5(4H)-one (P1) at 308 K

Inhibitor	Concentration (M)	R_S ($\Omega.cm^2$)	R_t ($\Omega.cm^2$)	CPE (μF)	n	C_{dl} ($\mu F.cm^{-2}$)	E_{Rt} (%)
1M HCl	-	1.93	14.50	298	0.88	200	-
Inhibitor (P1)	10^{-6}	3.61	71	238	0.80	92	80
	10^{-5}	5.75	106	214	0.79	87	86
	10^{-4}	5.15	137	174	0.78	41	89
	10^{-3}	5.73	439	67	0.81	35	97

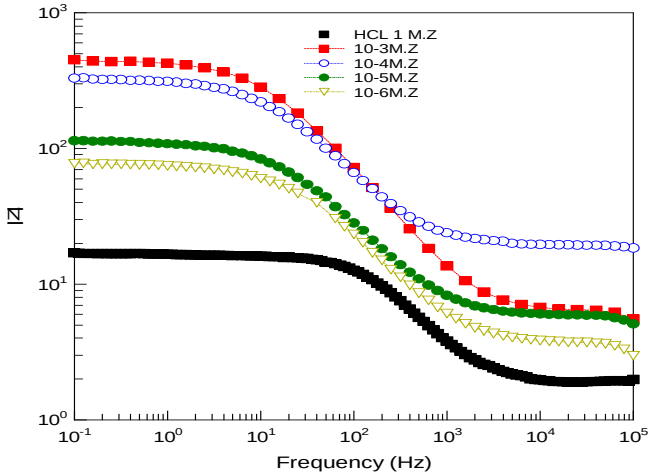

Figure 2. Bode plots of mild steel in 1 M HCl in the absence and presence of different concentrations of (E)-4-(2,3-Dihydro-1,3-benzothiazol-2-ylidene)-3-methyl-1-phenyl-1H-pyrazol-5(4H)-one (P1) at 308K

The capacitive behaviour of mild steel in presence of (E)-4-(2,3-Dihydro-1,3-benzothiazol-2-ylidene)-3-methyl-1-phenyl-1H-pyrazol-5(4H)-one **(P1)** could be visualized from Bode plots, also. An aggressive attack of HCl acid

corroded mild steel enormously and made surface highly irregular, which could be easily detected by small phase angle (Figures 2 and 3). On the contrary, adsorption of the (E)-4-(2,3-Dihydro-1,3-benzothiazol-2-ylidene)-3-methyl-1-phenyl-1H-pyrazol-5(4H)-one **(P1)** on mild steel effectively lowered surface irregularities, as a result phase angle increased approaching to 90°. This indicates increased capacity of the interface due to the presence of adsorbed inhibitor molecules at the interface.

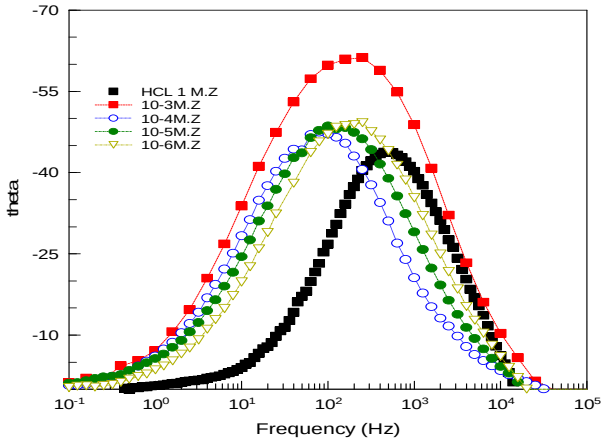

Figure 3. Phase angle plots of mild steel in 1 M HCl solution in the absence and presence of different concentrations of (E)-4-(2,3-Dihydro-1,3-benzothiazol-2-ylidene)-3-methyl-1-phenyl-1H-pyrazol-5(4H)-one (P1) at 308K

The impedance data obtained above were analyzed using an electrochemical equivalent circuit shown in Figure 4 where, R_s, R_{ct} and CPE stand for solution resistance, charge transfer resistance and constant phase element, respectively. The term CPE has been introduced to replace a double layer capacitance (C_{dl}) for more accurate fit [39]. The impedance of the CPE is defined as follows:

$$Z_{CPE} = Y^{-1}{}_0 (iw)^{-n} \quad \textbf{(8)}$$

Where Y_0 is a proportionality factor and 'n' has the meaning of phase shift. The value of 'n' represents the deviation from the ideal behavior and it lies between 0 and 1 [40]. The values of R_{ct} and CPE were obtained from the above mentioned equivalent circuit and are listed in Table 2. These data indicate that by increasing the concentration of (E)-4-(2,3-Dihydro-1,3-benzothiazol-2-ylidene)-3-methyl-1-phenyl-1H-pyrazol-5(4H)-one **(P1)**, the values of CPE tend to decrease and consequently E_{Rt} increases. The decrease in capacitance resulting from decrease of dielectric constant and/or an increase in the thickness of the electrical double layer suggests that (E)-4-(2,3-Dihydro-1,3-benzothiazol-2-ylidene)-3-methyl-1-phenyl-1H-pyrazol-5(4H)-one **(P1)** act by adsorption on the metal/electrolyte interface [41-42]. In the present case, it can be assumed that water molecules adsorbed on the surface of mild steel are replaced by (E)-4-(2,3-Dihydro-1,3-benzothiazol-2-ylidene)-3-methyl-1-phenyl-1H-pyrazol-5(4H)-one **(P1)**.

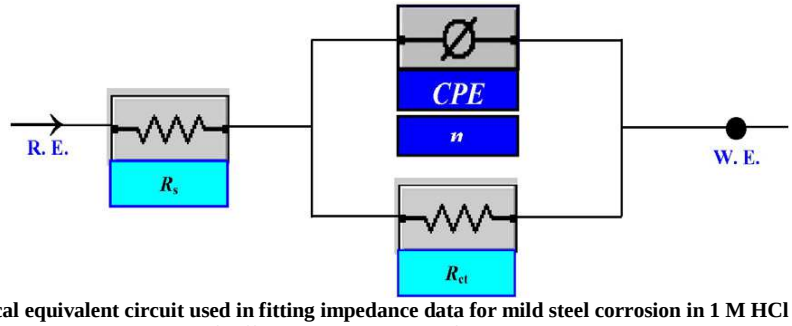

Figure 4. Electrochemical equivalent circuit used in fitting impedance data for mild steel corrosion in 1 M HCl in absence and presence of different concentration of studied system

3.2.1. Potentiodynamic Polarization Studies

Tafel data for mild steel immersed in 1 M HCl in the absence and presence of (E)-4-(2,3-Dihydro-1,3-benzothiazol-2-ylidene)-3-methyl-1-phenyl-1H-pyrazol-5(4H)-one **(P1)**, calculated from the curves in Figure 5 are given in Table 3. It is clearly seen from the figure 5 that both the anodic and cathodic curves shift to lower current densities on addition of inhibitor indicating retardation of anodic dissolution of mild steel as well as hydrogen ion reduction.

Electrochemical parameters show that the increase in concentration of (E)-4-(2,3-Dihydro-1,3-benzothiazol-2-ylidene)-3-methyl-1-phenyl-1H-pyrazol-5(4H)-one **(P1)** is associated with a displacement of corrosion potential towards more positive values. Additionally, inhibitor concentration affected the magnitude of Tafel slopes (ba and bc) and led to the profile where in b values changed irregularly in relation to the blank. The cathodic and anodic branches also did not uniformly shift with change in the concentration of (E)-4-(2,3-Dihydro-1,3-benzothiazol-2-ylidene)-3-methyl-1-phenyl-1H-pyrazol-5(4H)-one **(P1)**. These salts decreased i_{corr} and shifted E_{corr} towards less negative values. The shift in E_{corr} values was lower than 85 mV in each case suggesting that inhibitor (E)-4-(2,3-Dihydro-1,3-benzothiazol-2-ylidene)-3-methyl-1-phenyl-1H-pyrazol-5(4H)-one **(P1)** is mixed type inhibitor [43-44].

Table 3. Electrochemical parameters of mild steel in 1M HCl solution without and with (E)-4-(2,3-Dihydro-1,3-benzothiazol-2-ylidene)-3-methyl-1-phenyl-1H-pyrazol-5(4H)-one (P1) at different concentrations

Inhibitor	Concentration (M)	E_{corr} (mV/SCE)	I_{corr} (µA/cm^2)	-βc (mV/dec)	βa (mV/dec)	E (%)
1M HCl	-	-465	1386	292	101	---
Inhibitor (P1)	10^{-6}	-476	231	213	86	83
	10^{-5}	-477	175	204	91	87
	10^{-4}	-473	114	193	108	92
	10^{-3}	-474	72	199	102	95

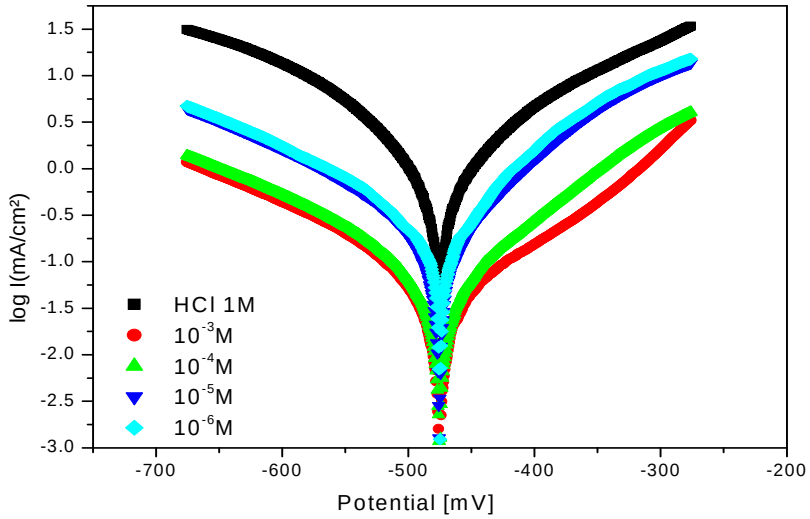

Figure 5. Potentiodynamic polarization curves of mild steel in 1M HCl in the presence of different concentrations (E)-4-(2,3-Dihydro-1,3-benzothiazol-2-ylidene)-3-methyl-1-phenyl-1H-pyrazol-5(4H)-one (P1)

3.2.2. Adsorption Isotherm

The efficiency of inhibitor molecules are related to their adsorption ability on the metal surface. An inhibitor reduces the corrosion rate by covering active centers on the metal surface. So, it is important to determine surface coverage ratio value (θ) for discussing the corrosion rate properly Figure 6, the linear relationships of C/θ versus C suggest that the adsorption of (E)-4-(2,3-Dihydro-1,3-benzothiazol-2-ylidene)-3-methyl-1-phenyl-1H-pyrazol-5(4H)-one **(P1)** on the mild steel is in well agreement with the Langmuir adsorption isotherm, which is expressed by the following equation.

$$\frac{C}{\theta} = \frac{1}{k} + C \qquad \textbf{(9)}$$

Where, C is the concentration of inhibitor, θ is surface coverage on the metal surface and K_{ads} is the equilibrium constant of adsorption process. The correlation coefficient (R^2= 0.999) was used to choose the isotherm that best fit experimental data.

The standard free energy of adsorption, $\Delta G°_{ads}$ is related to the K_{ads} with the equation given below:

$$K = \frac{1}{5555}\exp\left(-\frac{\Delta G^0_{ads}}{RT}\right)$$

The average value of the K_{ads} is 6.47 10^5 M^{-1} which reflects the high adsorption ability of the P1 molecules on the mild steel surface (Thermodynamic parameters were determined from gravimetric). The $\Delta G°_{ads}$ is negative and high (-44.52 kJ mol^{-1}) indicates the strong interactions between the inhibitor molecules and the metal surface [45-48]. Generally, the standard free energy of adsorption values of -20 kJ mol^{-1} or less negative are associated with physical adsorption; those of -40 kJ mol^{-1} or more negative involves charge sharing or transfer between inhibitor molecules and metals (chemical adsorption)[49-51]. However, the adsorption of organic molecules on metal surfaces cannot be considered as purely physical or chemical phenomenon. In addition to the chemical adsorption, inhibitor molecules can also be adsorbed on metal surface via physical interactions. In this study, the $\Delta G°_{ads}$ is modestly closer to -40 kJ mol^{-1}. Therefore, it is concluded that chemical interactions should be dominant for the adsorption of the (E)-4-(2,3-Dihydro-1,3-benzothiazol-2-ylidene)-3-methyl-1-phenyl-1H-pyrazol-5(4H)-one **(P1)** molecules on the mild steel surface [51-52].

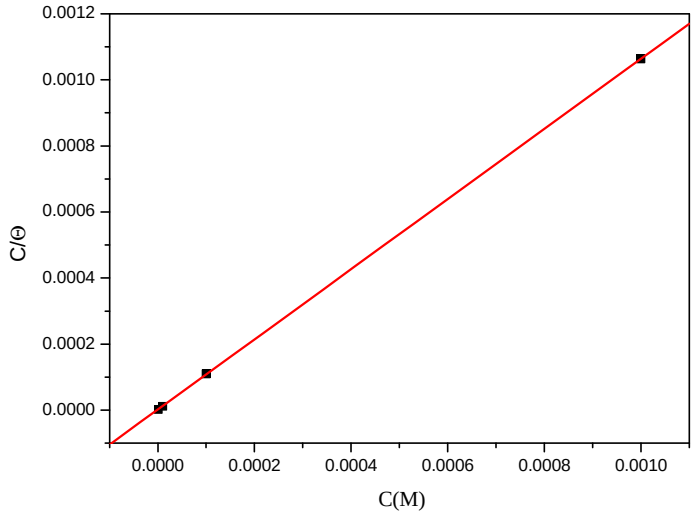

Figure 6. Langmuir isotherm plots for the adsorption of inhibitor on mild steel

3.3. Quantum chemical calculations

The quantum chemical calculations are performed on an Intel (R) core $(TM)_2$ Quad CPU (2.4 GHz and 8 GB RAM) computer using standard Gaussian-09 software package [53]. The geometries of the benzothiazol-pyrazole derivatives considered in this work are fully optimized, without any symmetry constraint at DFT level of theory using a B3LYP functional together with 6-31G(d,p) basis set in gaseous phase. Besides, for a better approach of the experimental parameters, the geometries are optimized in aqueous phase at the same level of theory using PCM model. The final optimized geometries are given in Figure 7 and the geometrical parameters values are presented in Table 4.

Table 4. Pertinent valence and dihedral angles, in degree, of the studied inhibitors calculated at B3LYP/6-31G(d,p) in gas, G and aqueous, A phases.

Angle	Phase	Value
$[C_7C_{13}C_{14}]$	G	134.20592
	A	133.18657
$[C_{16}N_{29}H_{30}]$	G	119.03165
	A	119.02650
$[S_{27}C_7C_{13}C_{14}]$	G	-0.00928
	A	0.00080
$[C_{17}C_{16}N_{29}H_{30}]$	G	0.01852
	A	0.02310

After the analysis of the theoretical results obtained, we can say that the molecule (E)-4-(2,3-Dihydro-1,3-benzothiazol-2-ylidene)-3-methyl-1-phenyl-1H-pyrazol-5(4H)-one **(P1)** have a planar structure. In fact, the benzothiazol, pyrazol and benzene rings are circa perpendicular to each other.

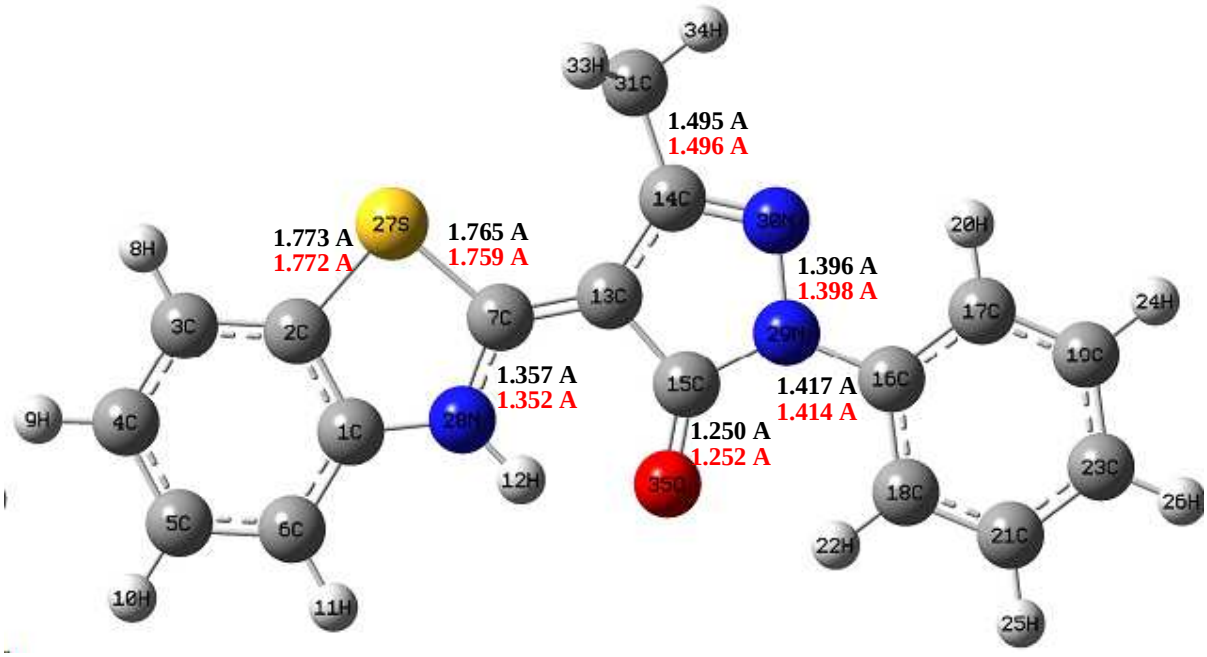

Figure 7. Optimized molecular structures and bond lengths of the studied inhibitors calculated in gas (black) and aqueous (red) phases at B3LYP/6-31G (d,p) level

Phase	TE (eV)	E_{HOMO}(eV)	E_{LUMO}(eV)	ΔE(eV)	μ(D)	IP(eV)	EA(eV)	χ	η
Gas	-35191.9	-5.321	-1.598	3.723	5.7259	5.321	1.598	3.460	0.931
Aqueous	-35194.8	-5.532	-1.603	3.929	8.3456	5.532	1.603	3.567	1.965

➢ **Local molecular reactivity**

Besides the global reactivity indicators, the analysis of atoms selectivity within inhibitors is very useful in indicating the reactive sites towards electrophilic and nucleophilic attacks. In the case of an electron-transfer for reaction control, the selectivity descriptors of choice are the condensed Fukui functions on atoms [54]. These descriptors inform about the veritable sites in a molecule on which nucleophilic, electrophilic or radical attacks are most likely possible.

In order to compute the condensed Fukui functions of a system of N electrons, we perform a

single point calculation of the anionic (N+1) and the cationic (N-1) species by using the neutral optimized geometry, at the same level of theory. The condensed Fukui functions are then computed using the finite-difference approximation as follow:

$$f_k^+ = P_k(N+1) - P_k(N)$$

$$f_k^- = P_k(N) - P_k(N+1)$$

$$f_k^0 = \frac{P_k(N+1) - P_k(N-1)}{2}$$

where, $P_k(N)$, $P_k(N+1)$ and $P_k(N-1)$ are the natural populations for the atom k in the neutral, anionic and cationic species respectively.

Tables 5 and 6 displays the most relevant values of the natural population (P(N), P(N-1) and P(N+1))

with the corresponding values of the Fukui functions (f_k^+, f_k^- and f_k^0) of the studied inhibitors. The calculated values of the f_k^+ for all inhibitors are mostly localized on the pyridine ring, namely S_{27}, N_{30} and O_{35} and C13, indicating that the pyrazolone and benzothiazole ring will probably be the favorite site for nucleophilic attacks.

Table 5. Pertinent natural populations and Fukui functions of the studied inhibitors calculated at B3LYP/6-31G(d,p) in gas (G) phase

Atom	Phase	P(N)	P(N+1)	P(N-1)	f^+	f^-	f^0
C_7	G	5,8810	6,0216	5,8888	0,1407	-0,0078	0,0664
C_{23}	G	6,2557	6,2866	6,1676	0,0310	0,0881	0,0595
S_{27}	G	15,5644	15,6849	15,4630	0,1206	0,1014	0,1110
N_{29}	G	7,2524	7,2547	7,1524	0,0024	0,1000	0,0512
N_{30}	G	7,2929	7,3809	7,2307	0,0881	0,0622	0,0751
O_{35}	G	8,6831	8,7479	8,5515	0,0648	0,1316	0,0982

Table 6. Pertinent natural populations and Fukui functions of the studied inhibitors calculated at B3LYP/6-31G(d,p) in aqueous (A) phase

Atom	Phase	P(N)	P(N+1)	P(N-1)	f^+	f^-	f^0
C_7	A	5,8770	6,0416	5,8826	0,1645	-0,0056	0,0795
C_{15}	A	5,3588	5,4350	5,3360	0,0762	0,0227	0,0495
S_{27}	A	15,5441	15,6996	15,4400	0,1555	0,1041	0,1298
N_{29}	A	7,2563	7,2591	7,1586	0,0028	0,0977	0,0503
N_{30}	A	7,3282	7,4020	7,2246	0,0738	0,1036	0,0887
O_{35}	A	8,7051	8,7722	8,5506	0,0671	0,1545	0,1108

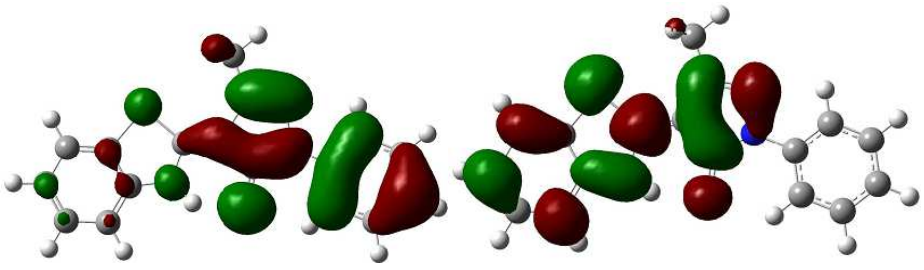

HOMO (G) LUMO (G)

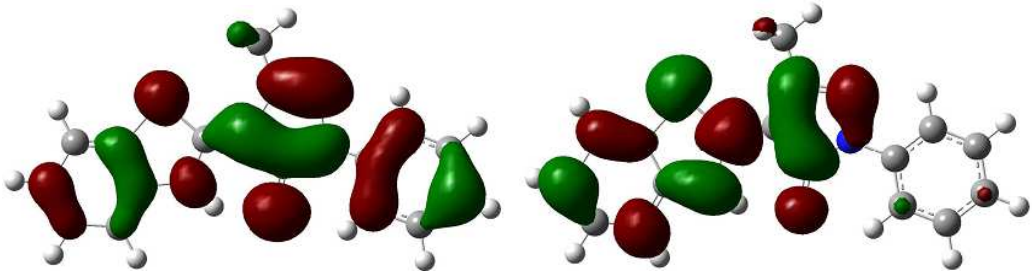

HOMO (A) LUMO (A)

Figure 8. The HOMO and the LUMO electrons density distributions of the studied inhibitors computed at B3LYP/6-31G(d,p) level in gas and aqueous phases

CONCLUSION

The corrosion inhibition mechanism and the stability of (E)-4-(2,3-Dihydro-1,3-benzothiazol-2-ylidene)-3-methyl-1-phenyl-1H-pyrazol-5(4H)-one **(P1)** on mild steel in 1 M HCl solution were investigated. According to the experimental findings, the following points could be concluded:

- (E)-4-(2,3-Dihydro-1,3-benzothiazol-2-ylidene)-3-methyl-1-phenyl-1H-pyrazol-5(4H)-one **(P1)** reduces the corrosion rate of mild steel in 1 M HCl solution. The inhibitory efficiency of this compound depends on its concentration.
- Polarization measurements show that (E)-4-(2,3-Dihydro-1,3-benzothiazol-2-ylidene)-3-methyl-1-phenyl-1H-pyrazol-5(4H)-one **(P1)** inhibit both the anodic and cathodic processes indicating that this is mixed type corrosion inhibitor.
- The corrosion of mild steel is mainly charge transfer controlled.
- The adsorption of all the (E)-4-(2,3-Dihydro-1,3-benzothiazol-2-ylidene)-3-methyl-1-phenyl-1H-pyrazol-5(4H)-one **(P1)** on the mild steel surface in HCl acid solution obeys the Langmuir adsorption isotherm.
- (E)-4-(2,3-Dihydro-1,3-benzothiazol-2-ylidene)-3-methyl-1-phenyl-1H-pyrazol-5(4H)-one **(P1)** molecules evenly distribute over the steel surface.

➢ The calculated parameters using quantum chemical equations correlated well with the experimental results.

REFERENCES

[1] H. Elmsellem, A. Aouniti, M. Khoutoul, A. Chetouani, B. Hammouti, N. Benchat, R.Touzani, M. Elazzouzi, *Journal of Chemical and Pharmaceutical Research*, **2014**, 6(4), 1216-1224.
[2] H. Elmsellem, N. Basbas, A. Chetouani, A. Aouniti, S. Radi, M. Messali, B. Hammouti, *Portugaliae. Electrochimica. Acta*, **2014**, 2, 77.
[3] H. Elmsellem, A. Elyoussfi, N. K. Sebbar, A. Dafali, K. Cherrak, H. Steli, E. M. Essassi, A. Aouniti and B. Hammouti, *Maghr. J. Pure & Appl. Sci*, **2015**, 1, 1-10.
[4] H. Elmsellem, A. Aouniti, Y. Toubi, H. Steli, M. Elazzouzi, S. Radi, B. Elmahi, Y. El Ouadi, A. Chetouani, B. Hammouti *, Der Pharma Chemica*, **2015**, 7, 353-364.
[5] A. Aouniti, H. Elmsellem, S. Tighadouini, M. Elazzouzi, S. Radi, A. Chetouani, B. Hammouti, A. Zarrouk, *Journal of Taibah University for Science*, **2015**, http://dx.doi.org/10.1016/j.jtusci.2015.11.008
[6]H. Elmsellem, K. Karrouchi, A. Aouniti, B. Hammouti, S. Radi, J. Taoufik, M. Ansar, M. Dahmani, H. Steli and B. El Mahi, *Der Pharma Chemica*, **2015**,7(10), 237-245.
[7] H. Elmsellem, T. Harit, A. Aouniti, F. Malek, A. Riahi, A. Chetouani , and B. Hammouti, *Protection of Metals and Physical Chemistry of Surfaces*, **2015**, 51(5), 873–884.
[8] H. Elmsellem, A. Aouniti, M.H. Youssoufi, H. Bendaha, T. Ben hadda, A. Chetouani, I. Warad, B. Hammouti, *Phys. Chem. News*, **2013**, 70, 84.
[9] H. Elmsellem, M. H.Youssouf, A. Aouniti, T. Ben Hadd, A. Chetouani, B. Hammouti. Russian, *Journal of Applied Chemistry*, **2014**, 87(6), 744−753.
[10] H. Elmsellem, H. Nacer, F. Halaimia, A. Aouniti, I. Lakehal, A .Chetouani, S. S. Al-Deyab, I. Warad, R. Touzani, B. Hammouti, *Int. J. Electrochem. Sci*, **2014**, **9**, 5328-5351.
[11] H. Elmsellem, A. Aouniti,M. Khoutou, A. Chetouani, B. Hammouti, N. Benchat, R. Touzani and M. Elazzouzi, J. *Chem. Pharm. Res*, **2014**, 6, 1216.
[12] H. Elmsellem, A. Elyoussfi, H. Steli, N. K. Sebbar, E. M. Essassi, M. Dahmani, Y. El Ouadi, A. Aouniti, B. El Mahi, B. Hammouti, *Der Pharma Chemica***, 2016**, 8(1), 248-256.
[13] H. Elmsellem, A. Elyoussfi, N. K. Sebbar, A. Dafali, K. Cherrak, H. Steli, E. M. Essassi, A. Aouniti and B. Hammouti, *Maghr. J. Pure & Appl. Sci*, **2015**, 1, 1-10.
[14] M. Boudalia, A. Bellaouchou, A. Guenbour, H. Bourazmi, M. Tabiyaoui, M.El Fal, Y. Ramli, E. M. Essassi, H. Elmsellem, *Mor. J. Chem*, **2014**, 2, 97.
[15] A. Elyoussfi, H. Elmsellem, A. Dafali, K. Cherrak, N. K. Sebbar, A. Zarrouk, E. M. Essassi, A. Aouniti, B. El Mahi and B. Hammouti, *Der Pharma Chemica*, **2015**, 7(10), 284-291.
[16] N. Saidi, H. Elmsellem, M. Ramdani, A. Chetouani, K. Azzaoui, F. Yousfi, A. Aounitia and B. Hammouti, *Der Pharma Chemica*, **2015**, 7(5),87-94.
[17] H. Elmsellem, H. Bendaha, A. Aouniti, A. Chetouani, M. Mimouni, A. Bouyanzer, *Mor. J. Chem*, **2014**, 2 (1), 1-9.
[18] N. K. Sebbar, H. Elmsellem, M. Boudalia, S. lahmidi, A. Belleaouchou , A. Guenbour, E. M. Essassi, H. Steli, A. Aouniti, *J. Mater. Environ. Sci*, **2015**, 6 (11), 3034-3044.
[19] H. Zarrok, H. Oudda, A. Zarrouk, R. Salghi, B. Hammouti, M. Bouachrine, *Der Pharm. Chem*, **2011**, 3 576.
[20] N. K. Sebbar, H. Elmsellem, M. Ellouz, S. Lahmidi, E. M. Essassi, I. Fichtali, M. Ramdani, A. Aouniti, A. Brahimi and B. Hammouti. *Der Pharma Chemica*, **2015**, 7(9):33-42.
[21] N. K. Sebbar, H. Elmsellem,M. Ellouz, S. Lahmidi, A.L. Essaghouani, E. M. Essassi ,M. Ramdani, A. Aouniti1, B. El Mahi and B. Hammouti. *Der Pharma Chemica*, **2015,** 7(10):579-587.
[22] H. Elmsellem, H. Nacer, F. Halaimia, A. Aouniti, I. Lakehal, A .Chetouani, S. S. Al-Deyab, I. Warad, R. Touzani, B. Hammouti, *Int. J. Electrochem. Sci*, **2014**, 9, 5328-5351.
[23] I. Hutchinson, S. A. Jennings, B. R. Vishnuvajjala, A. D. Wetsell, M. F. G. Stervens, *J. Med. Chem*, **2002**, 45, 744.
[24] T. D. Bradshaw, M. C. Bibby, J. A .Double, I. Fichtner, P. A. Cooper, M. C. Alley, S. Donohue, S. F. Stinson, J. E. T. Zewjski, E. A. Sausville & M. F. G. Steven, *.Mol. Cancer. Therapeutics*, **2002**, 1, 239.
[25] G. Manfroni , F. Meschini , M. L. Barreca , P. Leyssen , A. Samuele , N.Iraci , S. Sabatini, S. Massari , G. Maga , J. Neyts , V.Cecchetti, *Bioorganic & Medicinal Chemistry*, **2012**, 20, 866–876.
[26] A. Furlan, F Colombo, A. Kover, N. Issaly, C. Tintori ,L.Angeli, V. Leroux, S. Letard , M. Amat , Y. Asses ,B.Maigret , P. Dubreuil , M. Botta , R. Dono ,J. Bosch,O. Piccolo, D. Passarella , F.Maina, *European Journal of Medicinal Chemistry*, **2012**, 47, 239-254.
[27] F. Delmas, C. Digiorgio, M. Robin, N. Azas, M. Gasquet, C. Detang,M. Costa, P. T. David & J. P. Galy, *Antimicrob.Ag.Chemother*, **2002**, 46, 2588.
[28]L. Ouyang, Y. Huang , Y. Zhao , G. He, Y. Xie , J. Liu , J. He, B. Liu,Y. Wei, *Bioorganic & Medicinal Chemistry Letters*, **2012**, 22, 3044-3049.

[29] H. Moreno-Dı´az, R. Villalobos-Molina, R. Ortiz-Andrade, D. Dı´az-Coutin˜ o, J. Luis Medina-Franco,S. P. Webster, M. Binnie, S. Estrada-Soto,M. Ibarra-Barajas, I. Leo´n-Riverac and G. Navarrete-Va´zquez., *Bioorganic & Medicinal Chemistry Letters*, **2008**, 18, 2871–2877.
[30] P.Rathelot, N.Azas, H.El-kashef, F.Delmas, C.Di Giorgio, P.Timon-David, J.Maldonado, P.Vanelle. Eur.J.Med.Chem, **2002**, 42, 671-679.
[31] P.K.Sharma, S.Kumar, P.Kimar, P.Kaushik, D.Kaushik, Y.Dhingra, K.R.Aneja, *European J. of Med. Chem*, **2010**, 45, 2650-2655.
[32] B. Insuasty, A. Tigreros, F. Orozco, J. Quiroga, R. Abonia, M. Nogueras, A. Sanchez, J. Cobo, *Bioorganique & Médical Chim*, **2010**, 18, 4965-4974.
[33] I. Chakibe, A.Zerzouf, E. M. Essassi, M. Reicheltd & H. Reuterd, *Acta Cryst*, **2010**, E66, o1096.
[34] A.D. Becke, *Chem. Phys*, **1993**, 98, 5648.
[35] A.D. Becke, *Phys. Rev. A*, **1988**, 38, 3098.
[36] C. Lee, W. Yang, R.G. Parr, *Phys. Rev. B*, **1988**,37, 785.
[37] W. Wang, W.J. Mortier, *J. Am. Chem. Soc*, **1986**,108, 5708.
[38] C.C. Zhan, J. A. Nichols, D.A. Dixon, *J.Phys.Chem. A*, **2003**,107, 4184.
[39] K.B. Samardzija, C. Lupu, N. Hackerman, A.R. Barron, A. Luttge, A. Inhibitive, *Corros. Sci*, **2009**, 51, 595–601.
[40] H.N. Shubha, T.V. Venkatesha, K. Vathsala, M.K. Pavitra, M.K.P. Kumar, *ACS Appl. Mater. Interfaces*, **2013**, 5,10738–10744.
[41] X. Wang, H. Yang, F. Wang, *Corros. Sci*, **2011**, 53, 113–121.
[42] Y. El Ouadi, H. Elmsellem, M. El Fal, N. K. Sebbar, A. Bouyanzer, R. Rmili, E. M. Essassi, B. El Mahi, L. Majidi & B. Hammouti, *Der Pharma Chemica*, **2016**, 8(1), 365-373.
[43] A. Anejjar, A. Zarrouk , R. Salghi , D. Ben Hmamou, H. Zarrok, S. S. Al-Deyab, M. Bouachrine, B. Hammouti, N. Benchat. Int. J. Electrochem. Sci, **2013,** 8, 5961-5979.
[44] H. Elmsellem, A. Elyoussfi, N. K. Sebbar, A. Dafali, K. Cherrak, H. Steli, E. M. Essassi, A. Aouniti and B. Hammouti. Maghr. J. Pure & Appl. Sci, **2015**, 1, 1-10.
[45] G. Avcı, *Mater. Chem. Phys*, **2008**,112, 234-238.
[46] Tayebi H.Himmi B. Ramli Y., Zarrouk A., Geunbour A., Bellaouchou A.,Zarrok H.,Boudalia M., El Assyry M., *Res. J. Pharm., Biol. Chem. Sci*, **2015**, 6, 1861.
[47] M.A. Quijano, M.P. Pardav, A. Cuán, M. R. Romo, G. N. Silva, R. Á. Bustamante, A.R. López, H.H. Hernández, *Int. J. Electrochem. Sci.*, **2011**, 6, 3729.
[48] M.J. Bahrami, S.M.A. Hosseini, P. Pilvar, *Corros. Sci*, **2010**, 52, 2793-2803.
[49] X. Wang, H. Yang, F. Wang, *Corros. Sci*, **2011**, 53, 113-121.
[50] N.A. Negm, Y.M. Elkholy, M.K. Zahran, S.M. Tawfik, *Corros. Sci*, **2010**,52, 3523-3536.
[51] X. Li, S. Deng, H. Fu, *Corros. Sci*, **2011,** 53, 302-309.
[52] I. Ahamad, R. Prasad, M.A. Quraishi, *Corros. Sci*, **2010**, 52, 3033-3041.
[53] Gaussian 09, Revision **E.01**, M. J. Frisch, G. W. Trucks, H. B. Schlegel, G. E. Scuseria, M. A. Robb, J. R. Cheeseman, G. Scalmani, V. Barone, B. Mennucci, G. A. Petersson, H. Nakatsuji, M. Caricato, X. Li, H. P. Hratchian, A. F. Izmaylov, J. Bloino, G. Zheng, J. L. Sonnenberg, M. Hada, M. Ehara, K. Toyota, R. Fukuda, J. Hasegawa, M. Ishida, T. Nakajima, Y. Honda, O. Kitao, H. Nakai, T. Vreven, J. A. Montgomery, Jr., J. E. Peralta, F. Ogliaro, M. Bearpark, J. J. Heyd, E. Brothers, K. N. Kudin, V. N. Staroverov, R. Kobayashi, J. Normand, K. Raghavachari, A. Rendell, J. C. Burant, S. S. Iyengar, J. Tomasi, M. Cossi, N. Rega, J. M. Millam, M. Klene, J. E. Knox, J. B. Cross, V. Bakken, C. Adamo, J. Jaramillo, R. Gomperts, R. E. Stratmann, O. Yazyev, A. J. Austin, R. Cammi, C. Pomelli, J. W. Ochterski, R. L. Martin, K. Morokuma, V. G. Zakrzewski, G. A. Voth, P. Salvador, J. J. Dannenberg, S. Dapprich, A. D. Daniels, Ö. Farkas, J. B. Foresman, J. V. Ortiz, J. Cioslowski, and D. J. Fox, Gaussian, Inc., Wallingford CT, 2009.
[54] K. Fukui, T. Yonezawa, H. Shingu, *J. Chem. Phys.*, **1952**, 4, 722-725.